UNIVERSITY OF CALIFORNIA,

IRVINE

Engineering a Cellular Assay for DNA-Encoded Library Screening

THESIS

submitted in partial satisfaction of the requirements for the degree of

MASTER OF SCIENCE

in Biomedical Engineering

by

Jeffrey Nam Lam

Thesis Committee:

Professor Brian M. Paegel, Chair

Professor Abraham Lee

Professor Tim Downing

2022

Table of Contents

LIST OF FIGURES

ACKNOWLEDGEMENTS

I would like to thank all those who were a part of this journey. Specifically, I wish to thank my committee chair, Professor Brian Paegel for all his guidance in becoming a better researcher, scientist, and person. I also wish to thank Professors Timothy Downing, Abraham Lee, Robert Spitale and Elliot Hui for insight on the biomedical field and fostering my love for the research being done at UC Irvine. Thank you to Val Cavett, who has been the backbone of this project and a life mentor to me, and Angela Torres, who has taught me much about mentorship. A special thanks to the members of the Paegel lab, especially Juan Hu, Patrick Fitzgerald, Anjali Dixit, and Huda Barhoosh, who have always supported me and will make invaluable contributions to the scientific community. Finally, thank you to my parents, who have shown me unconditional love throughout my life.

ABSTRACT OF THE THESIS

Engineering a Cellular Assay for DNA-Encoded Library Screening

By

Jeffrey Lam

Master of Science in Biomedical Engineering

University of California Irvine, 2022

Professor Brian M. Paegel, Chair

High-throughput screening is the foundation for modern small molecule discovery, but DNA-encoded library (DEL) technology has emerged as an alternative approach to synthesizing and screening large collections for novel bioactive chemical matter. Currently, DEL screening is limited to affinity selection binding assays and, more recently, biochemical activity-based assays. This thesis describes the engineering of a cellular DEL activity assay that can serve as the basis for DEL screening on live cells. DEL beads were modified to support growth of cells and report on cellular activity using standard cellular reporter assays. Design of this platform took into account cell phototoxicity, cell viability and growth, and design of a model cellular signal transduction assay. This thesis successfully demonstrates proof-of-concept compatibility of the developed cellular assay with solid-phase DEL chemistry, paving the way for cellular phenotypic DEL screening technology.

Chapter 1: INTRODUCTION

The combination of high-throughput screening and DNA-encoded libraries (DEL) has made its mark on pharmaceutical drug discovery, producing lead molecules and clinical candidates from this partnership [1,2]. DELs use affinity selection- that is, evaluating library members through incubation with a protein target and designating most active binders as hits 2-combined with modern sequencing to create a diverse and robust assay platform with low costs and expanded chemical matter [3]. Libraries are prepared via split-and-pool synthesis, where resin beads are partitioned into separate wells, coupled to a building block, encoded using DNA ligation unique to each well, pooled, and resplit until the desired member diversity is achieved. With at least 10^3 reactions per cycle, one split-and-pool cycle will lead to a library size of 10^6, and even higher diversity is easily achieved when combined with modern automation technology. Overall this platform is an integration of current gold standard technologies and can be applied to many targets.

Affinity selection binding assays are the conventional mode of DEL analysis, but droplet microfluidics has emerged as a means of enabling activity-based DEL screening. DEL beads are encapsulated in microfluidic water-in-oil droplets of activity assay reagent. The encapsulated beads undergo a series of integrated microfluidic manipulations, including photochemical library member cleavage from the bead, incubation, fluorescence-based assay detection, and droplet sorting [4]. This technology has been used to screen for inhibitors of autotaxin (ATX), a phosphodiesterase, and the receptor tyrosine kinase (RTK) discoidin domain receptor I (DDR1), both of which are implicated in disease pathways such as cancer and autoimmune diseases [5,6]. In a model ATX screen, droplets are loaded with a DEL bead, ATX, and fluorogenic ATX substrate, which fluoresces when cleaved by ATX. Inhibitors of ATX therefore attenuate fluorescence signal in droplet, and droplets below a certain threshold are sorted as hits. DNA

from hit beads is then amplified and sequenced to determine the structure of molecules responsible for inhibition.

While biochemical activity-based DEL screening holds promise for new target classes, the clinical and physiological relevance of any biochemical hit still requires validation in cells. In vitro cell-based DEL assays could provide a more disease-relevant target of screening while also identifying liabilities, such as cytotoxicity. There is no current technology available for conducting cellular assays on DELs.

Directly integrating cells in the current microfluidic droplet-based screening paradigm poses several significant challenges. Droplet encapsulation of single beads and cells is dogged by the low probability of double occupancy as calculated by the Poisson distribution [7,8]. Additionally, adherent cells suspended in a water-in-oil emulsion without proper media conditions, CO_2 levels, and humidity will not be viable past ~ 1 h.

We choose to depart from droplet microfluidics and instead use a microcarrier approach to dodge the limitations of droplet tissue culture and screening via microcarrier technology. Microcarriers are high-surface-to-volume microscale spheres that are functionalized for cell adhesion and growth [9]. Industrially, microcarriers are used for rapid cell proliferation, but are merely substrates for culture. In our approach, the DEL beads are transformed into microcarriers by functionalizing them with cellular adhesion promoters, which allow cells to grow around the bead in a confluent monolayer. Classical DEL screening then applies with library members being liberated via photocleavage. A library member then interacts with the surrounding cells. The cells are engineered to transduce target activity (e.g. receptor activation, transcription factor binding, etc.) through secretion of an affinity-tagged fluorescent protein. The microcarrier DEL bead is also functionalized with the affinity tag ligand, permitting putative proximity-driven capture and concomitant bead labeling with the secreted reporter.

As a proof-of-concept cellular assay target, we selected the cGAS-STING pathway, an immune response pathway implicated in tumorigenesis[10]. Cell-based screens targeting the

STING pathway have identified several agonists. Amongst those was MSA-2, which we chose as our model agonist [11]. Commercial STING pathway reporter cells (293-Dual hSTING-R232, InvivoGen) have been engineered to report STING activity via release of secreted embryonic alkaline phosphatase (SEAP). SEAP activity is detected by adding culture media to the profluorescent SEAP substrate fluorescein diphosphate (FDP). This robust and straightforward control assay served as the foundation for our efforts to add our own custom reporters to the cell line.

At the conclusion of this project, we show the design of custom DEL microcarriers with the ability to seed cells, photocleave off model agonist, and capture a fluorescent reporter from the seeded cells. Implementing this approach, adaptation of the activity-based DEL screening concept to a cellular signal transduction assay was pursued to demonstrate cell viability, comparable photocleavage efficiency, and DNA compatibility. Future work on this project will involve engineering a cell line that can secrete a Halotag-labeled fluorescent protein that can be captured on the microcarrier, confirming that photocleaved STING ligand successfully induces secretion and capture on the ligand DEL bead, and finally, determining culture conditions suited to DEL screening.

Chapter 2: Microcarrier Design for DEL-compatibility and Cell Growth

Our cell-based DEL screening approach drew significant inspiration from activity-based biochemical screening. In the typical microfluidics assay, beads are loaded into droplets with target protein and substrate, compound is cleaved via UV, compound and target are incubated together, and finally fluorescence activated droplet sorting occurs. Aspects of this methodology were preserved during adaptation of cell-based screening protocols **(Fig 1)**. First, reporter cells are seeded onto microcarriers and left to culture (24 h) until confluence. Then, compartmentless UV dosage in incubator is done at the hour time scale, notably different from the instantaneous exposure in circuit done in the microfluidic version. Incubation and exposure are integrated into the same step, and analysis is done by FACS, which is very high throughput (>10 kHz). Each step required careful investigation for integration.

In order to move the DEL assay to a live cell format, we focused on bead functionalization and emulation of commercial microcarrier design. Concurrent work in the lab on Cytodex I microcarriers suggested how DEL beads could be functionalized and seeded for use as microcarriers [12,13]. These microcarriers are typically used for expansion of stem cells, and so in an industry setting there are production scale up protocols that would be relevant to our application [14]. In preliminary studies, we decided to culture in 96-well plates, allowing higher throughput testing and manageable cell counts for a laboratory setting.

Commercial microcarriers were an excellent testbed for establishing culture conditions, but lacked the functions we desired for detecting signaling. We modified DEL beads with a polyacrylamide shell coat to introduce various functionalities under very mild conditions. Ammonium persulfate (APS) is added to aqueous solution containing DEL beads, acrylamide, and bisacrylamide monomers, while N,N,N’,N’-tetramethylethylenediamine (TEMED) is added to a separate oil solution. APS and TEMED catalyze polyacrylamide polymerization. By layering

Figure 1. Workflow for cellular DEL screening. Reporter cells (yellow) are seeded onto gelatin-coated DEL bead microcarriers and cultured. Following growth to confluence, compound is photocleaved to dose cells with each DEL member. DEL bead microcarriers are retrieved, cells are washed off gently using pipette disaggregation, and DEL microcarriers are sorted by FACS. During dosing, microcarriers capture HaloTag-labeled fluorescent protein reporter secreted by cells responding to the microcarrier. DNA encoding tags are then amplified and sequenced (PCR, NGS) to determine the identity of hits.

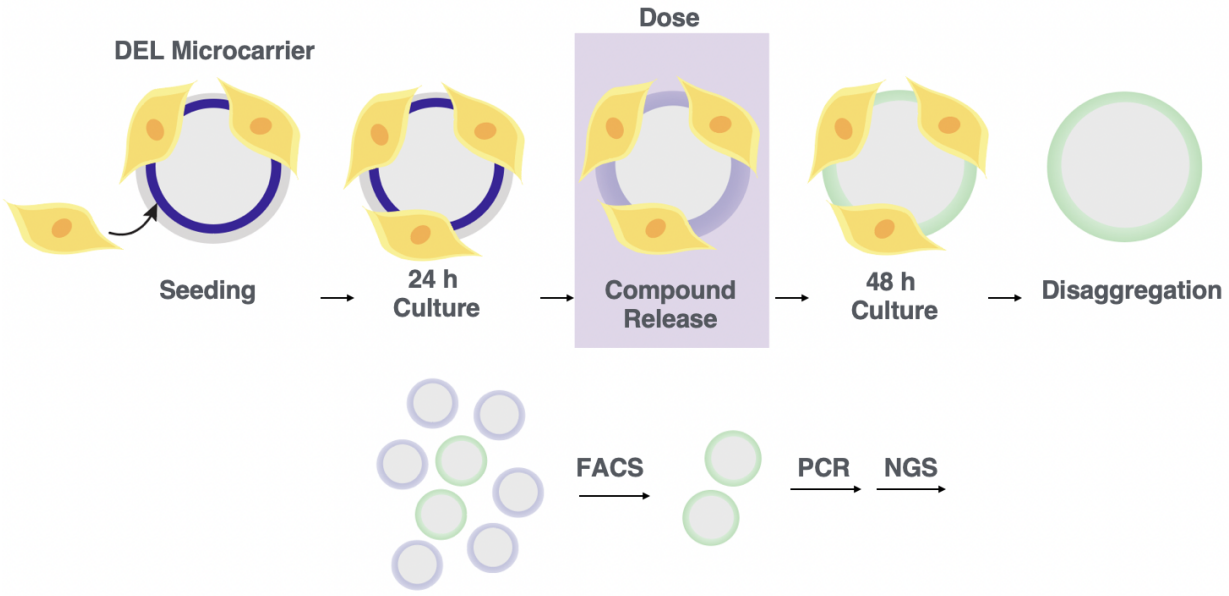

the oil over the aqueous layer and creating an emulsion with high speed agitation, droplets form around the DEL beads that are several microns larger in diameter than the beads [15,16]. Using a beadbug tissue homogenizer, acrylamide droplets containing APS in the aqueous droplets surrounded by oil containing TEMED are formed. The polymer shells are cured under oxygen-free conditions (to prevent quenching of the radical-mediated polymerization), yielding DEL beads with a polyacrylamide shell coat **(Fig 2)**. Bulk emulsification was preferred over microfluidic droplet encapsulation due to superior throughput- over 1 million beads were processed per sample and four samples could be simultaneously processed at our lowest throughput, meaning the limiting factor becomes the DEL beads and not the emulsification. We also bypass optimization and fabrication of a microfluidic device suited for encapsulation of both cells and DEL beads. Droplet size uniformity is not a concern as the gel shell is templated by the uniform tentagel bead [17].

The polyacrylamide shell is a versatile scaffold for displaying myriad functionality for detecting cell signals and promoting cell adhesion and proliferation. Stiffness of the polyacrylamide can be adjusted based on monomer concentration, which is useful to adjust for cell seeding, since cells need very specific surface conditions for seeding. Additionally, a methacrylated protein can be incorporated into the polyacrylamide crosslinked backbone, meaning surface modifications with cellular adhesion molecules for seeding or acrydite primers for probe hybridization and confirmation of polyacrylamide layer is possible [18,19]. Also included in the polyacrylamide layer was the chloroalkane HaloTag capture ligand, which covalently binds to the HaloTag reporter protein. Various reporter proteins can be fused with the HaloTag for capture onto the microcarrier [20,21].

Promoting cell adhesion and growth on DEL beads was a key early concern. A literature search on cell mechanobiology and adhesion studies yielded a list of cellular adhesion molecules, many of which were extracellular matrix proteins [22,23,24]. Methacrylated versions of these proteins were obtained in an attempt to incorporate them into the polyacrylamide gel

Figure 2. Preparation of DEL bead microcarriers for cellular assay. Polyacrylamide is first incorporated through a bulk water-in-oil emulsification with acrylamide/bisacrylamide monomer (A:B) and reaction in the presence of APS/TEMED. Gelatin is then shell-coated via a 10% gelatin soak for 24 h and then incubation with genipin crosslinker for 48 h.

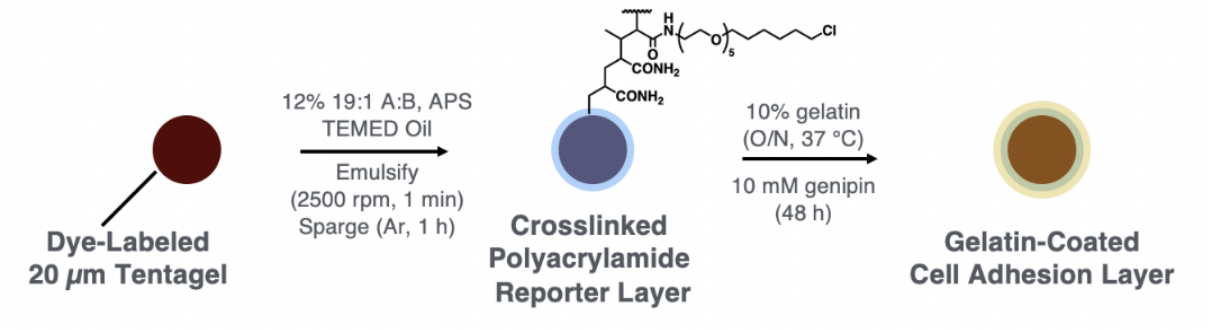

reporter scaffold, however necessary concentrations could not be achieved for seeding, as increasing the concentrations of these adhesion proteins led to solidified mixtures.

We instead used bifunctional linkers to bond the collagen covalently onto the already crosslinked polyacrylamide surface. Collagen was linked to the gel via sulfo-SANPAH **(Fig 3A)**, a heterobifunctional linker with a nitrophenyl azide group that photoreacts to insert into N-H sites on the acrylamide chains following a UV exposure [25,26]. The N-hydroxysuccinimide (NHS) ester of sulfo-SANPAH then reacts with primary amines on collagen. Another method was incorporation of a primary amine, 3-aminopropyl methacrylamide (APMA), into the polyacrylamide backbone allowed a homobifunctional linking using disuccinimidyl suberate (DSS) to react with primary amines on both the microcarrier and collagen in solution **(Fig 3B)**. Finally, gelatin crosslinking was explored. Following a 24 h incubation, gelatin was aspirated out and replaced with 10 mM genipin, which crosslinks the primary amines on gelatin [27,28] **(Fig 3C)**. Residual gelatin soaked into the porous polyacrylamide and TentaGel resin was enough to form a thin gelatinized layer on the microcarrier following a 24 h incubation in the genipin. Confirmation of gelatin is indicated by a bead color change to blue, which increases in intensity as crosslinking increases [29].

Despite the most consistent results, the UV exposure necessary for sulfo-SANPAH linkage was ultimately incompatible with our method, as DEL members going through linkage would photocleave, leading to loss of bead payload. APMA copolymerization followed by DSS does not require a UV active step, but results were more inconsistent, as DSS is insoluble in DI H_2O and requires at least 10% DMSO to solubilize. Since DMSO can induce apoptosis in cells, we were not able to find stable reaction conditions. Gelatin microcarriers were seeded consistently and induced cell adhesion and confluent growth. Colorimetric confirmation of gelatin crosslinking was also vital in developing a seeding quality control checkpoint.

With gelatin, our DEL microcarriers are adapted for cell adhesion and growth. Copolymerization of APMA into the polyacrylamide backbone also shows the flexibility of

Figure 3. Mechanisms of adhesion layer formulation. Several methods were attempted before arriving at gelatin coating as the cell adhesion strategy. **A** Conventional cell adhesion strategies use Sulfo-SANPAH as a bifunctional linker, which reacts with collagen lysine chains. **B** Homobifunctional linker disuccinimidyl suberate (DSS) mediates coupling of collagen to amino side chains in the acrylamide. **C** Gelatin is soaked into the porous tentagel beads, and soaked gelatin is then crosslinked using genipin. Micrographs of cell seeding using each approach are shown at right. Scale = 50 μm

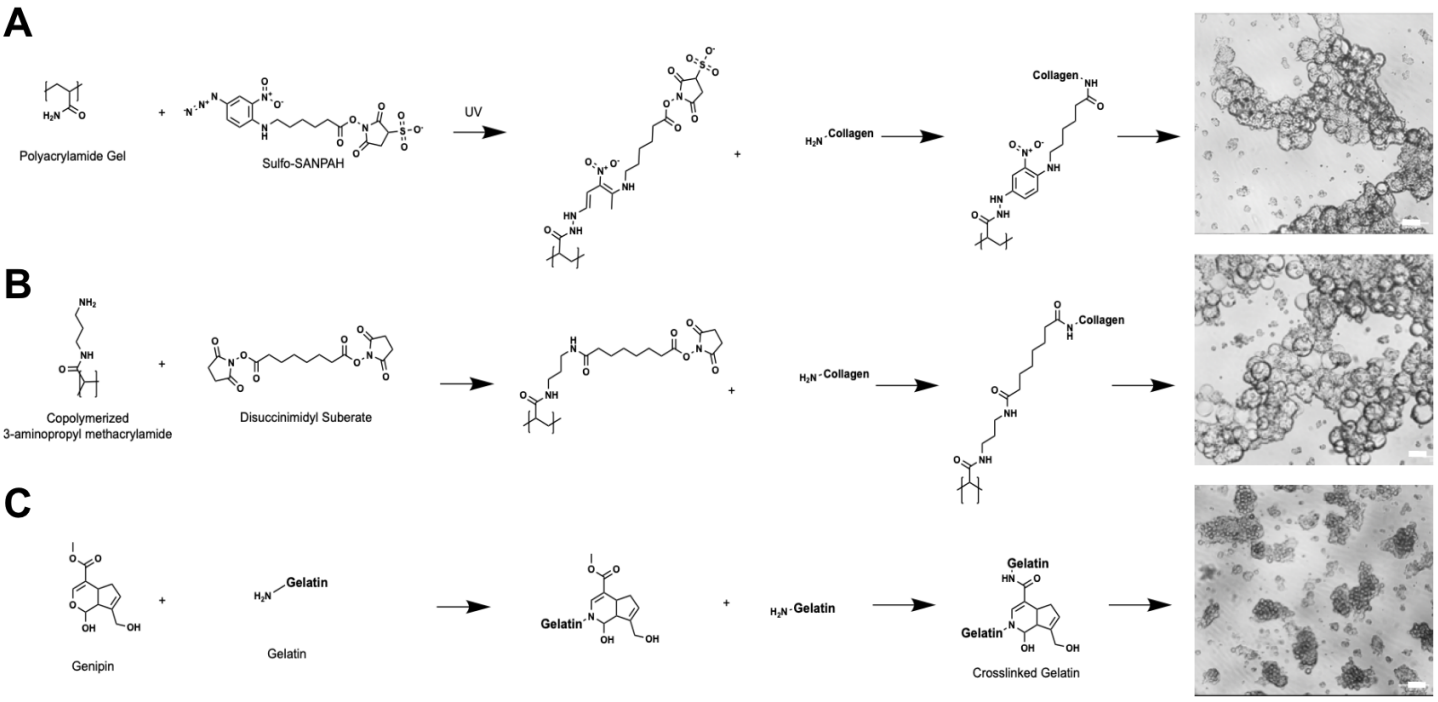

backbone structure given that the desired molecule is methacrylated. With the wide array of molecules able to be displayed by our microcarriers, we can adapt this method for different cell lines that may prefer a protein other than collagen or a stiffer scaffold. With translation of the DEL bead to microcarriers, it is now necessary to manipulate the seeding method to obtain a phenotype where cells do not interact with multiple microcarriers and distinct microcarrier-cell “compartments” are formed.

Chapter 3: Live Cell Assay Design

After establishing microcarrier preparation and culture conditions, cellular activity assay conditions were explored. In the microfluidic version, droplet compartments are used to partition the beads into monodisperse droplets. The DEL bead is fully exposed to the protein of interest in droplet, and any liberated compound will interact with the protein target. UV irradiation liberates compound (365 nm). Liberated compound is confined to the droplet. In our cell-based assay, we explored the feasibility of compartmentless conditions, involving only the microcarrier surrounded by a confluent monolayer of cells and the liberated compound.

Evaluation of photorelease focused on the amount of compound liberated and viability of cells after photoexposure. In the microfluidic compartment assay, a 10-μm bead displays 10^{-15}-10^{-19} moles of compound, and when liberated, doses at 100-300 μM. Photocleavage of fluorescein (FAM) coupled onto DEL beads with a photolabile linker (PC-FAM) **(Fig 4A)** quantifies our photorelease efficiency based on a fluorimetric assay of post-exposure supernatant. In order to increase payload, we decided to move from 10-μm resins to 20-μm resins. A photocleavage study was conducted using an Analytik Jena UVP Crosslinker oven (365 nm, **Fig 4B**). Both types of resins were irradiated (1 h), and bead supernatant was collected throughout. Based on this data, we also calculated the concentration of FAM within a 10 μm radius of the microcarrier, a simplified measurement of what cells might experience when photocleavage occurs.

Figure 4. Photocleavage evaluation for 10-μm vs 20-μm resins. **A** The structure of the photocleavable fluorescein (PC-FAM) bead is shown, with the green indicating the FAM molecule that is cleaved off when exposed to UV light (365 nm). **B** Concentration of cleaved FAM as a function of UV irradiation time was determined. The concentration of FAM experienced in the 10-μm volume surrounding the microcarrier was also calculated (right axis).

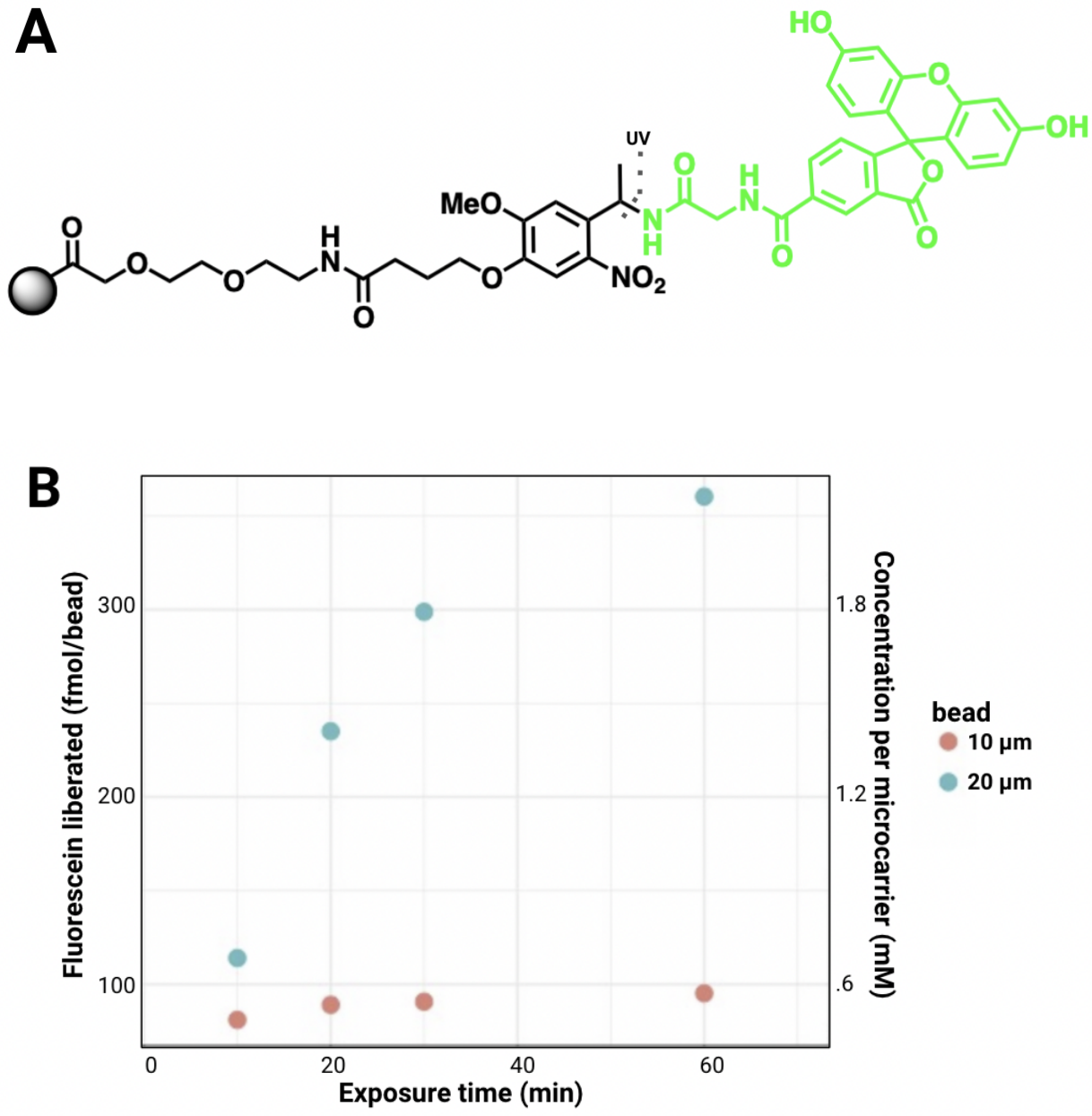

Over 1 h, 20-μm resins released over four times as much compound as their 10-μm counterparts, and when converting that to microcarriers estimated at 60-μm diameter, a concentration of over 2 mM dosage is predicted. This was done by dividing the amount of FAM liberated by microcarrier volume. However, this is an instantaneous measurement based on a plate assay, while in the actual microcarrier culture experiment, compound will be continually emanating from the bead and diffusing into the bulk solution, where it will be at too low a concentration to induce other cells. Based on these calculations, we expect a low dosage exposure over 24 h to give sufficient concentrations. Studies examining this will be discussed in the model dosing.

Further alteration of exposure methods were necessary to account for cell viability. Several studies have shown that 365-nm light is not necessarily cytotoxic at 1-2 min time spans but can induce DNA damage [30,31]. We adjusted our UV treatment method based on studies that indicated longer wavelengths can be less cytotoxic and still be within the excitation range of our photolinkers [32]. Additionally, treatment in circuit is done using a high power 365 nm laser. We posit that dosing via lower intensity, higher wavelength irradiation will improve viability. Our solution came in the form of commercial decorative UV LED strip lights, which according to manufacturers emit at 385-400 nm. These lights were a preferred option for low intensity controlled dosing in incubator.

Cytotoxicity studies were done to compare the UV LEDs to the UV oven. Six well plates of HEK293 cells were exposed to either the UV oven or with UV LED strips wrapped around (1 h), and then stained with two viability stains, Calcein AM and Live-Or-Dye, and analyzed via FACS **(Fig 5A)**. Additionally, in order to substitute the 365 nm laser photocleavage method, the light strip LEDS have to be able to photocleave the nitrophenyl photolabile linker and release the payload compound into solution. In order to quantitate, we photocleaved previously described PC-FAM beads [33] and compared photocleavage supernatant fluorescence from either

the UV oven or in the UV-LED equipped incubator **(Figs 5B-C)**. Lastly, a UV-vis spectrum was acquired to determine the most efficient wavelength for photocleavage.

Cytotoxicity of both UV oven and UV-LED light strip irradiation was determined using standard cell viability reagents. After 1 h exposure, viability was less than 25% for the UV oven exposure condition. Viability of cells exposed to the highest possible intensity of UV LED light strips remained at 95%, similar to the live cell population.

Based on our results, the light strip LEDs do not compromise cell viability and still liberate sufficient compound via photocleavage. Photocleavage efficiency via UV-LED was lower, likely because the UV-vis spectrum indicated that while the photolabile linker absorbs at 385-400 nm, molar absorptivity is much lower than at the peak excitation wavelength of 350 nm. Despite this, photocleavage of FAM is observed, and lower photocleavage efficiency is not a concern since we desire to dose over longer times. In the end, we settled on UV LEDs for our dosing method due to uncompromised viability and comparable photocleavage efficiency. Microcarrier cell seeding next required study. Production level microcarrier usage occurs in large spinner flasks ranging anywhere from 50 mL to 10 L, with laboratory settings opting for 50-100 mL [34]. One million 20-μm beads only take up 4 μL, and so in these design trials, we opted for culture in 96-well plates. For a better understanding of cell seeding on microcarriers, confocal microscopy live cell imaging was used to observe seeding for 24 h. A 1:10 ratio of gelatin functionalized microcarriers to HEK293 cells was mixed in a 70 uL live cell imaging dish, and put into a temperature-and humidity-controlled chamber (37 ^{o}C, 5% CO_2, **Fig 6**). Images were taken every 5 min and compiled to observe changes in cell and microcarrier position and attachment. Cells formed attachments to the microcarriers within 2 h. At 24 h, aggregates are seen, with cells forming attachments with each other at 5 h.

We decided that to decrease aggregate formation, microcarriers with cells attached would be put in agitation culture following 2 h of cell seeding. Through this, we achieve a majority of singlet microcarriers with attached cells, and though aggregates still exist, they are

Figure 5. Evaluation of LED light strips for viability and photocleavage efficacy. **A** Commercial UV light strips (385 nm) show cell viability very similar to unexposed live cells after 1 h while exposure at 365 nm causes death in the majority of the population. Error bars reflect SDOM (N=6). **B** Over a time-course of 6 h, UV LED light strips performed similarly though lower in magnitude to photocleavage in the UV oven. **C** A UV-Vis spectrum of the photocleavable linker used for DEL synthesis shows lower but appreciable absorption at 380-400 nm. **D** UV LED lights are adapted into the tissue culture incubator for irradiation of cells under optimal culture conditions (37 °C, 5% CO_2).

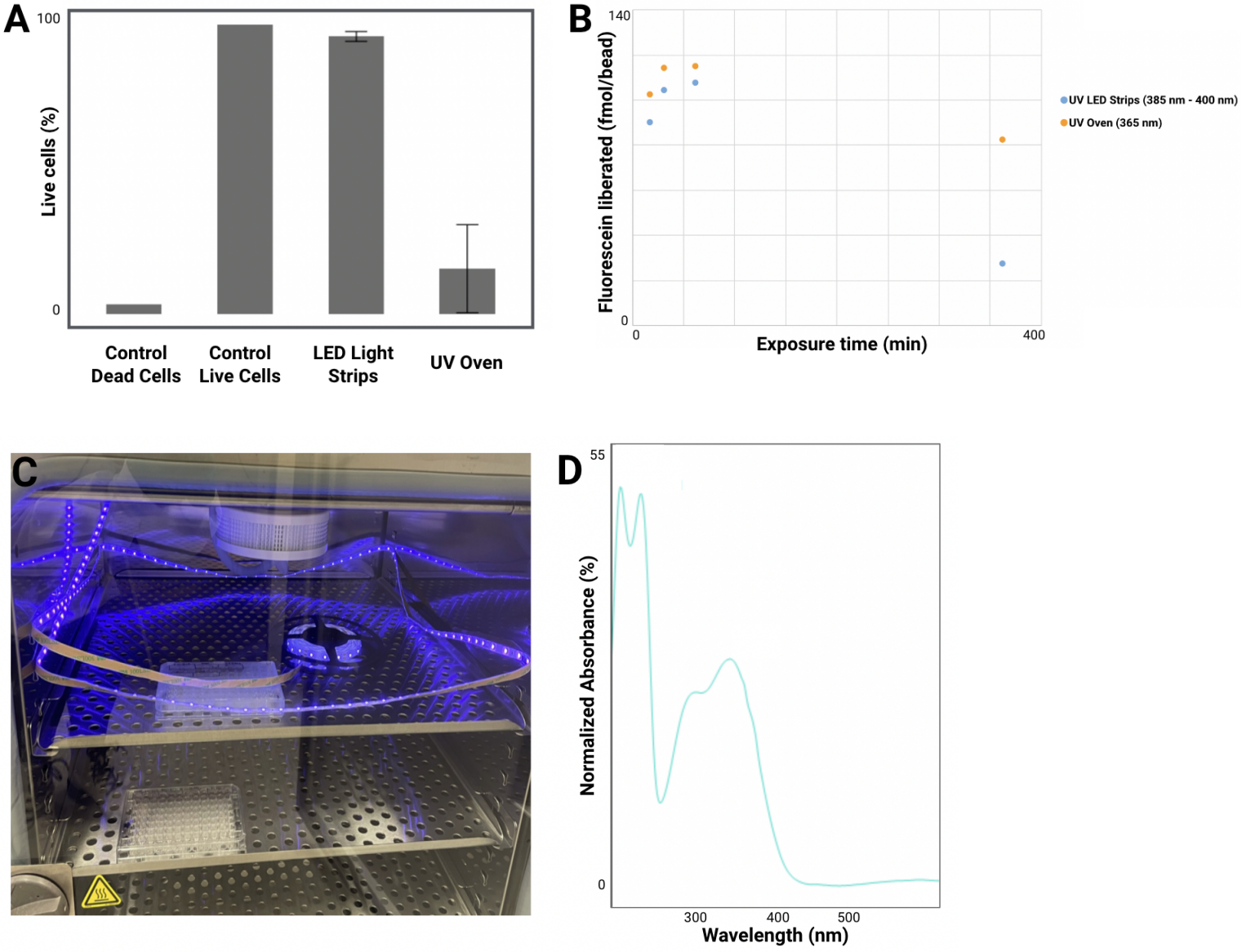

Figure 6. Live cell time-course imaging of microcarrier seeding. Confocal imaging of cell and microcarrier mixing was performed from 0 - 17 h (37 ºC, 5% CO_2). At 0 h, some microcarriers (teal) are close to one another and cells (green) are spread throughout. At 2 h, cells begin attaching to both microcarriers and other cells, forming a network. At 14 h, cells have formed a monolayer around the microcarriers and are ready for photodosing. Scale = 100 µm

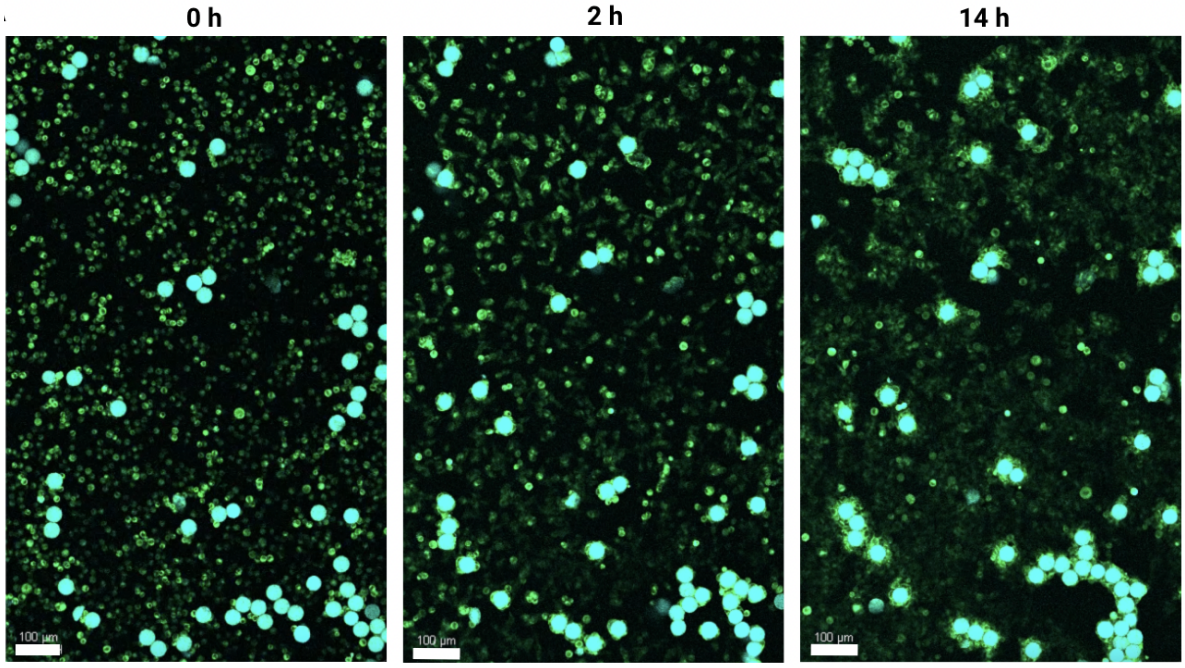

on the scale of 3-5 microcarriers and not more than 50. These results show that we have established a method for microcarrier cell seeding that minimizes aggregate formation and lets us evaluate at a low volume scale.

We next engineered a cell line to adapt affinity based screening to a cell-based assay. We looked to engineer a reporter cell line that secretes a HaloTag-labeled fluorescent protein (Halo-FP) upon stimulation with a ligand of the protein of interest **(Fig 7A)**. As a model, we engineered a cell line that constitutively secretes Halo-FP to establish a baseline for capture before moving onto an inducible line. This was done through CRISPR/Cas9 gene editing [35]. The plasmid for stable cell line generation contained a CAG promoter, antibiotic resistance gene for selection into a stable cell line, and GFP-HaloTag (GFP-Halo) fusion reporter protein **(Fig 7B)** [36]. This sequence was inserted into the adeno-associated virus integration site 1 (AAVS1) locus, a "safe harbor." [37]. Media was taken from stably transfected cells and compared to bacterially expressed and purified GFP-Halo. A HaloTag ligand appended tetramethylrhodamine (TMR) was used to bind the GFP-Halo product as well as purified GFP-Halo, and fluorescent gel scans were taken to confirm binding **(Fig 7C)**. Culture media was also evaluated for fluorescence compared to that of wild-type HEK293s, with the engineered line media showing much greater GFP fluorescence **(Fig 7D)**.

With the cell line verified, we next sought to demonstrate reporter capture on microcarriers. First, the chloroalkane HaloTag ligand was integrated on microcarrier by acrylating the ligand and incorporating it into the polyacrylamide backbone. We procured a amine-functionalized HaloTag ligand, and through a coupling of methacrylic acid using EDC and NHS carbodiimide crosslinking chemistry, we synthesized HaloTag ligand-methacrylate (**Fig 8A)**. Microcarriers with this in-house ligand crosslinked to the polyacrylamide backbone were then assayed via flow cytometry to show GFP-Halo capture **(Fig 8B)**. Microcarriers containing the ligand (+Halo) incubated with 5 μM GFP-Halo showed 10X fluorescence compared to negative control.

Figure 7. Reporter cell signaling schematic and cell line design. **A** Reporter cells are engineered such that receptor engagement with ligand induces expression of a secreted fluorescent protein - HaloTag fusion reporter (e.g. GFP-Halo). The DEL microcarrier surface, which is functionalized with HaloTag ligand, becomes labeled with GFP-Halo through covalent binding of HaloTag and its ligand. **B** A model reporter cassette for stable transfection includes a chromatin insulators that block silencing of reporter gene expression, constitutive CAG promoter, WPRE element to enhance gene expression, and bovine growth hormone polyadenylation sequence (bghPolyA) for transcription termination. A hygromycin resistance marker is also included for selection. The P2A self-cleaving peptide separates the reporter gene from the resistance marker. **C** Gel analysis verified that GFP-Halo secreted from engineered HEK293s bound to HaloTag ligand. L=Ladder, 1=Recombinantly produced GFP-Halo, 2=Recombinantly produced GFP-Halo + TMR-Ligand, 3=HEK293 secreted GFP-Halo, 4= HEK293 secreted GFP-Halo + TMR-Ligand. **D** Fluorescence analysis of culture media from wild-type HEK293 versus culture media from stably transfected secreted GFP-Halo (secGFP-Halo) reporter line. Error bars reflect SDOM (N=3).

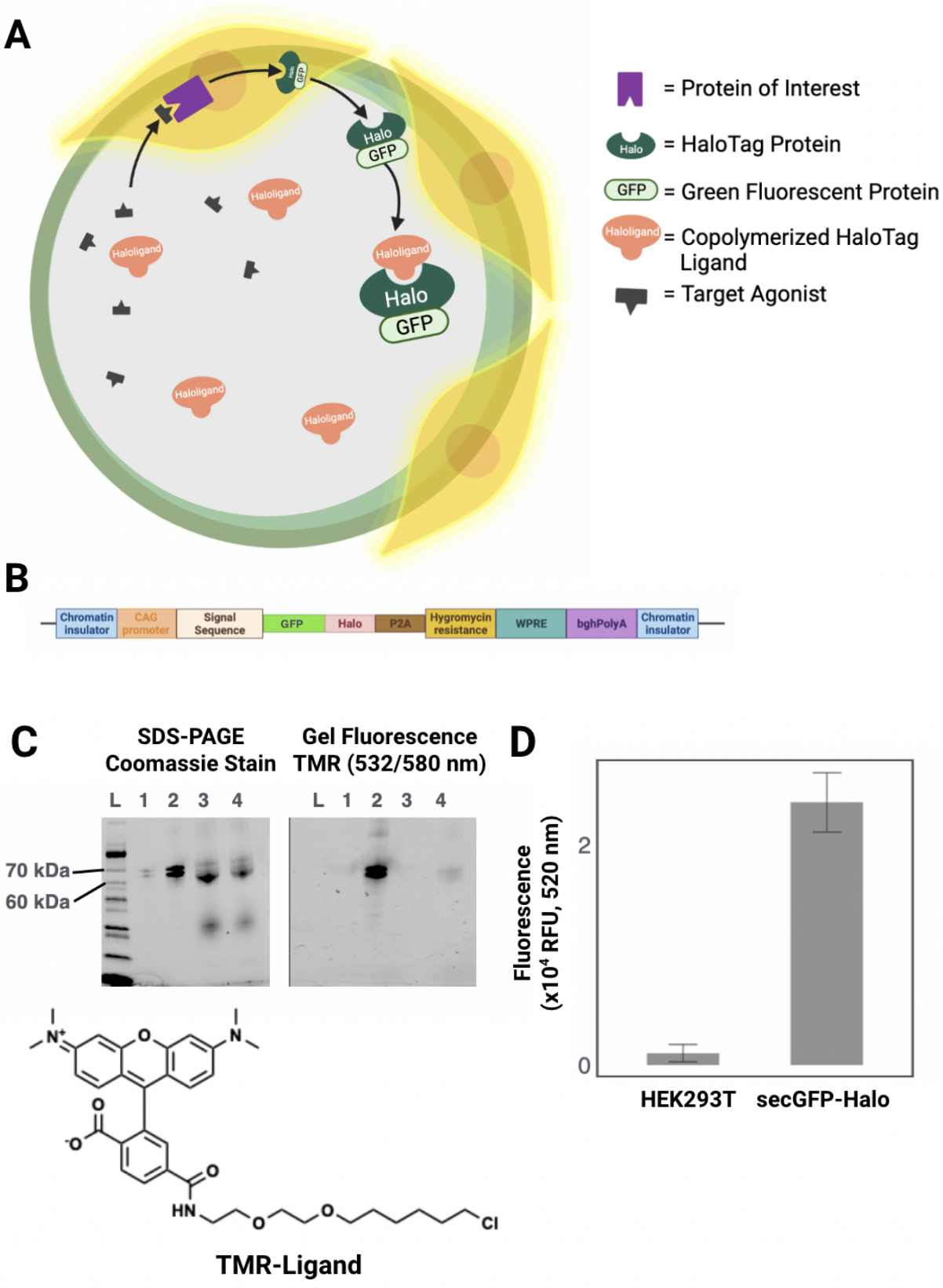
A
Halo
GFP
Haloligand
= Protein of Interest
= HaloTag Protein
= Green Fluorescent Protein
= Copolymerized HaloTag Ligand
= Target Agonist
B
Chromatin insulator
CAG promoter
Signal Sequence
GFP
Halo
P2A
Hygromycin resistance
WPRE
bghPolyA
Chromatin insulator
C
SDS-PAGE Coomassie Stain
Gel Fluorescence TMR (532/580 nm)
L 1 2 3 4
70 kDa
60 kDa
TMR-Ligand
D
Fluorescence (x10⁴ RFU, 520 nm)
2
0
HEK293T
secGFP-Halo

Figure 8. HaloTag ligand synthesis and characterization. HaloTag ligand was prepared with an amino NH_2-ligand starting material. Reaction with methacrylic acid (MAA) in the presence of EDC and NHS yielded a methacrylamide analog of the HaloTag ligand for copolymerization into the polyacrylamide matrix. **B** Microcarriers functionalized with the HaloTag ligand were reacted with recombinantly expressed and purified GFP-Halo and analyzed by flow cytometry. Controls included no HaloTag-ligand (-Halo) and no GFP-Halo(-GFP) treatment.

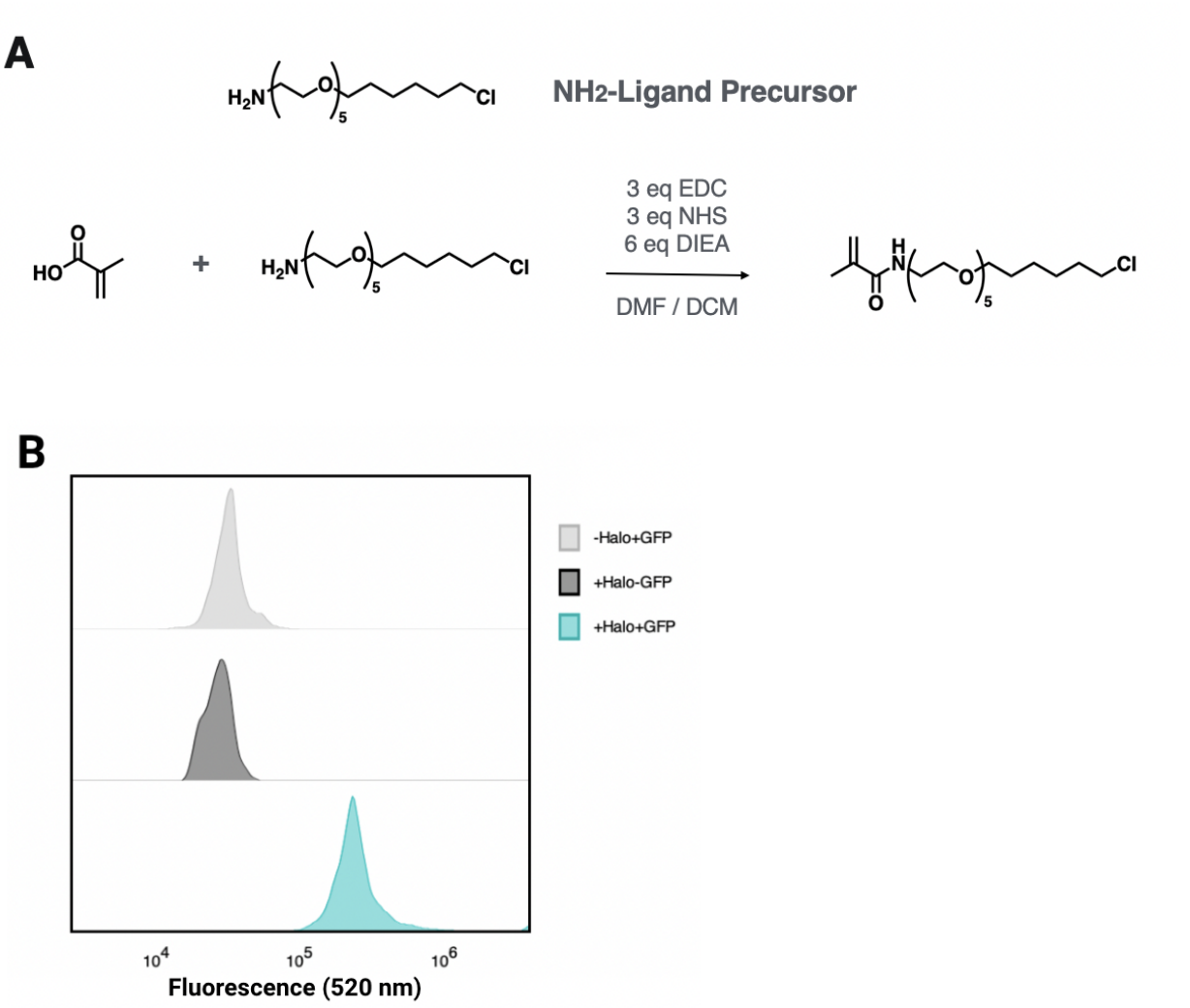

This experiment establishes that the microcarrier can capture HaloTag protein using the copolymerized chloroalkane HaloTag ligand. We have modified the parameters of the microfluidic activity-based DEL assay to a live cell platform. We established UV photocleavage exposure parameters to improve cell viability while maintaining effective photocleavage efficiency. Furthermore, we adjusted cell seeding conditions so singlet microcarriers with attached cells could be obtained. Finally, we developed a Halo-FP reporter secreting cell line and showed capture of purified Halo-FP on microcarriers using a custom in house methacrylated HaloTag ligand. With these data, our final proof-of-concept experiment is now in sight: demonstration of microcarrier capture of secreted reporters.

Chapter 4: Proximity-Driven Capture and Model Assay

As a culmination of this project, we show that microcarriers can capture GFP-Halo from engineered constitutively GFP-Halo secreting cell lines, and that cells on microcarriers experience a photocleaved payload from the microcarriers. In doing this, we revisit the idea of the compartmentless assay and evaluate whether bead-to-cell signaling and cell-to-bead signaling are possible. To do this, we establish that a proximity-driven effect exists where microcarriers seeded with constitutively GFP-Halo secreting cells show GFP-Halo capture but microcarriers in the presence of media from culture with constitutively GFP-Halo secreting cells do not show capture. Lastly, to model dose, we require an inducible cell line that can secrete GFP-Halo upon stimulation with a known agonist. Lacking that cell line, we modeled our dosing using 293-Dual hSTING-R232 cells on microcarriers and exposing them to a known STING agonist, MSA-2. A response from these cells to photocleavable MSA-2 payload microcarriers would show that bead-to-cell signaling is possible, and nearly complete our validation.

We hypothesize based on literature that a proximity effect exists where our microcarriers will capture reporter from the cells even though this reporter would quickly move into the bulk solution. Past publications have shown that bioluminescent split reporters produced by two different cells showed no interaction at far distances (30 mm) but interact and fluoresce when the cells are 1 mm apart [38]. We can maximize the upper and lower limits distance-wise using our microcarrier system. Attached cells are, by definition, on the microcarrier, and so the lower limit is set at 0 while the upper limit when the cell product goes into the bulk is on a much higher length scale. This effect is likely possible as the concentration in bulk is much lower, and so a microcarrier should not capture protein from the bulk, but should capture protein from cells within its monolayer.

To test this effect, we seeded HaloTag ligand displaying gelatin functionalized microcarriers with constitutively GFP-Halo secreting cells and non-fluorescent cells. After incubation for 48 h, microcarriers were disaggregated from cells and fluorescence was quantified with flow cytometry **(Fig 9)**. These data were compared with microcarriers without HaloTag ligand functionality to prove whether capture was occurring or if GFP was remaining on the microcarrier due to other reasons. Microcarriers seeded with GFP-Halo cells seeded on showed >10X magnitude in fluorescence compared to the microcarriers seeded with non fluorescent hSTING R232 cells. Additionally, microcarriers seeded with GFP-Halo cells without the HaloTag ligand copolymerized did not show a fluorescence profile shift, indicating that HaloTag mediated capture occurs for our HaloTag ligand functionalized microcarriers.

We next wanted to understand whether this capture was occurring due to the cells being grown on the microcarrier or not, demonstrating a proximity-driven effect. We establish the concentration limits present in the proximity effect and what we expect our microcarrier to be experiencing in terms of signal concentration by treating HaloTag ligand displaying microcarriers with purified GFP-Halo concentrations ranging from .01-10 μM and examining fluorescence using flow cytometry **(Fig 10)**. Microcarriers exposed to a concentration of 10 nM to 316 nM showed similar fluorescence profiles, while microcarriers exposed to 10 μM showed a 100X difference in fluorescence from untreated. With this range, we applied our data from the secreted capture experiment to show that while bulk media concentration from culture with constitutively secreting GFP-Halo secreting cells is around 20 nM after 48 h incubation, the microcarriers with fluorescent cells on them experience a reporter concentration of more than 1 μM based on comparison to our concentration titration curve.

Based on this experiment we conclude that a proximity effect may exist where microcarriers exposed to bulk media show no fluorescence profile shift, yet microcarriers with seeded fluorescent cells will experience a much higher concentration and show a shift. A 100-fold increase in concentration from .01-1 μM is necessary for a fluorescence profile shift on

Figure 9: Secreted reporter capture using seeded reporter cells. Either stably transfected constitutive secreted GFP-Halo HEK293 cells (293GFP) or nonfluorescent 293-Dual hSTING-R232 cells (hSTING) were cultured on both HaloTag ligand functionalized (+Halo) and naive (-Halo) microcarriers. After 48 h, microcarriers were disaggregated and analyzed by flow cytometry.

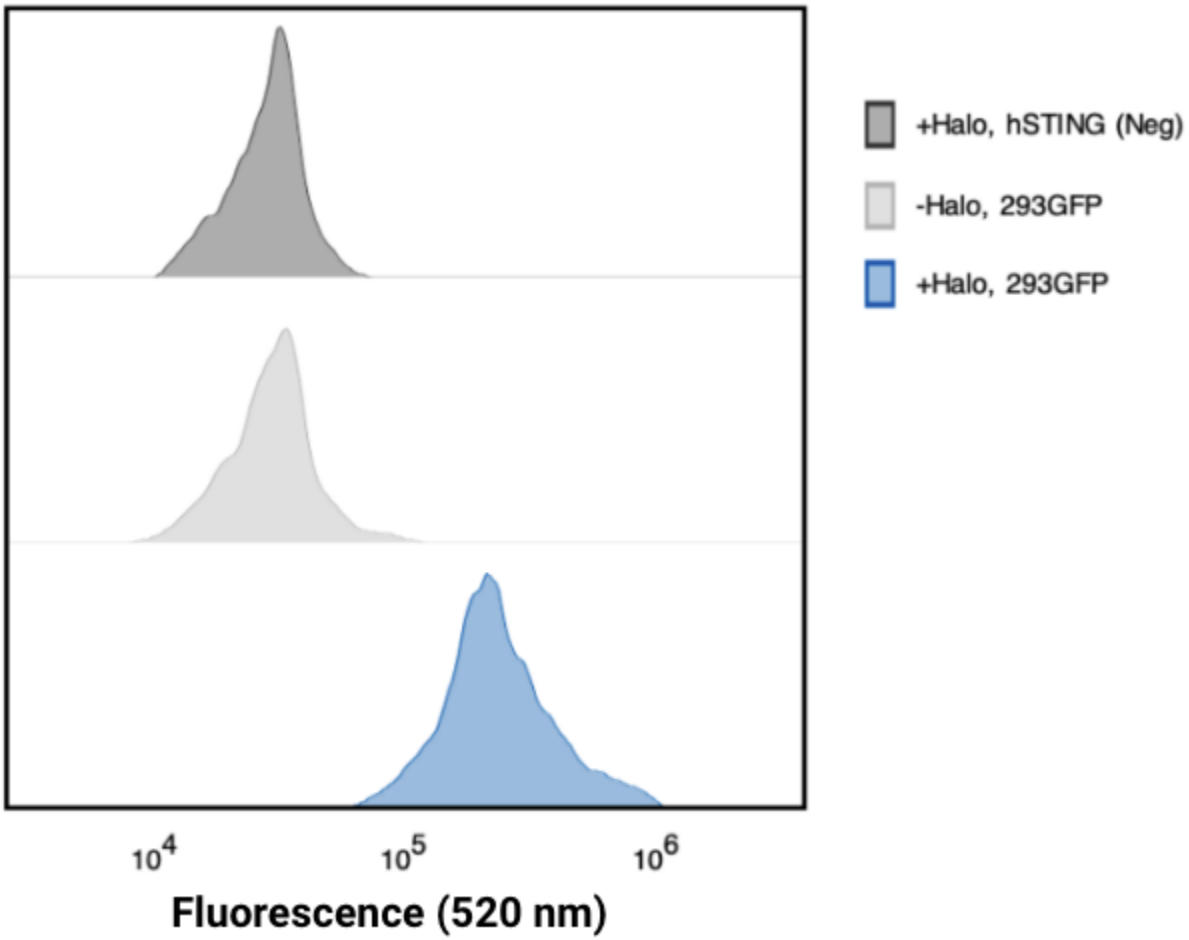

Figure 10: Proximity-driven capture of secreted GFP-Halo on microcarriers. HaloTag ligand-functionalized microcarriers were treated with known concentrations of purified GFP-HaloTag (.01 - 10 μM.) Additionally,microcarriers were seeded and cultured (48 h) with constitutively secreted GFP-HaloTag cells (secreted capture). Microcarriers were analyzed by flow cytometry.

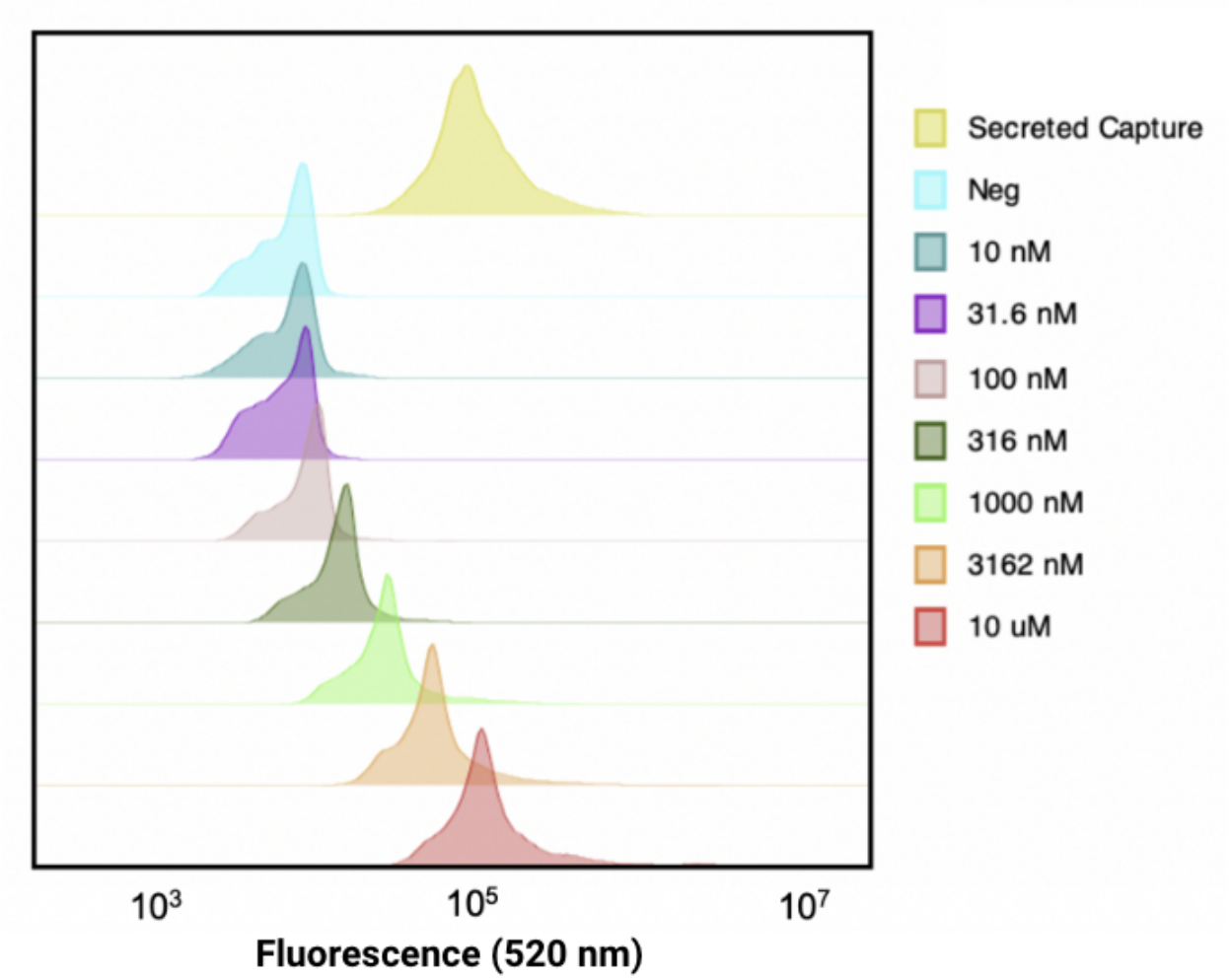

FACS. Since this range is covered between seeded microcarriers and unseeded microcarriers in fluorescent supernatant, we anticipate compartmentless cell-to-bead signaling is possible.

Now that cell-to-bead signaling has been shown, our last limitation is demonstrating bead-to-cell signaling and that a DEL bead is compatible with cell treatments. We accomplished this through use of 293-Dual hSTING R232 cells and model STING agonist, MSA-2. In choosing a model agonist, we required a molecule with DEL synthesis-compatible chemistry as well as no adverse chemistry when exposed to the assay protocol. Several known agonists such as DMXAA showed photochemical decomposition when exposed to 385 nm UV [39]. MSA-2's carboxylic acid lends itself to esterification with an alcohol group. We conductedSteglich esterification, where dicyclohexylcarbodiimide (DCC) and dimethylaminopyridine (DMAP) are used to activate the carboxylic acid and generate an active auxiliary to catalyze transesterification, respectively. Using a secondary alcohol displaying photolabile linker, we conduct this reaction and confirm on-bead product formation **(Fig 11A)** using matrix-assisted laser desorption/ionization time of flight mass spectrometry (MALDI-TOF) [40]. We then showed that MSA-2 does not undergo spurious photochemistry. MSA-2 was dissolved into aqueous solution and irradiated with UV LEDs (1 h). LC-MS analysis of our treated MSA-2 showed no side product formation and similar spectra to that of the untreated purified product **(Fig 11B).** Lastly, we seeded microcarriers containing photocleavable MSA-2 (PC-MSA-2) with R232 cells, grew to confluence for 24 h, photodosed at 385-400 nm with UV LED lights for 1 h, cultured for 24 h, and collected media for analysis. Fluorescence was measured with FDP, a SEAP substrate. After 2 h, media from the irradiated cells showed high fluorescence similar to positive control cells treated with 10 μM MSA-2, while media from cells grown on microcarriers and not UV treated showed low fluorescence similar to negative control blank media **(Fig 11C)**.

Since fluorescence of media from cells on irradiated PC-MSA-2 beads was high, SEAP was present to cleave FDP into FAM, and SEAP production only occurs when the cells are exposed to a STING agonist, thus confirming that the bead can signal to cells. Additionally, the

Figure 11. Photocleavable MSA-2 validation in cellular activity assay. **A** Structure of a photocleavable MSA-2 (PC-MSA-2) hSTING agonist. **B** PC-MSA-2 was UV irradiated by the UV LED light strips (1 hr). Untreated (left) and UV irradiated PC-MSA-2 (right) bead supernatant was analyzed by LC-MS. **C** 293-Dual hSTING-R232 cells were seeded and cultured on PC-MSA-2 microcarrier beads. Samples were either UV irradiated via UV LED (385-400 nm) or left untreated. Media was analyzed for SEAP activity and compared with media from reporter cells induced with MSA-2 (positive control) or untreated cells (negative control).

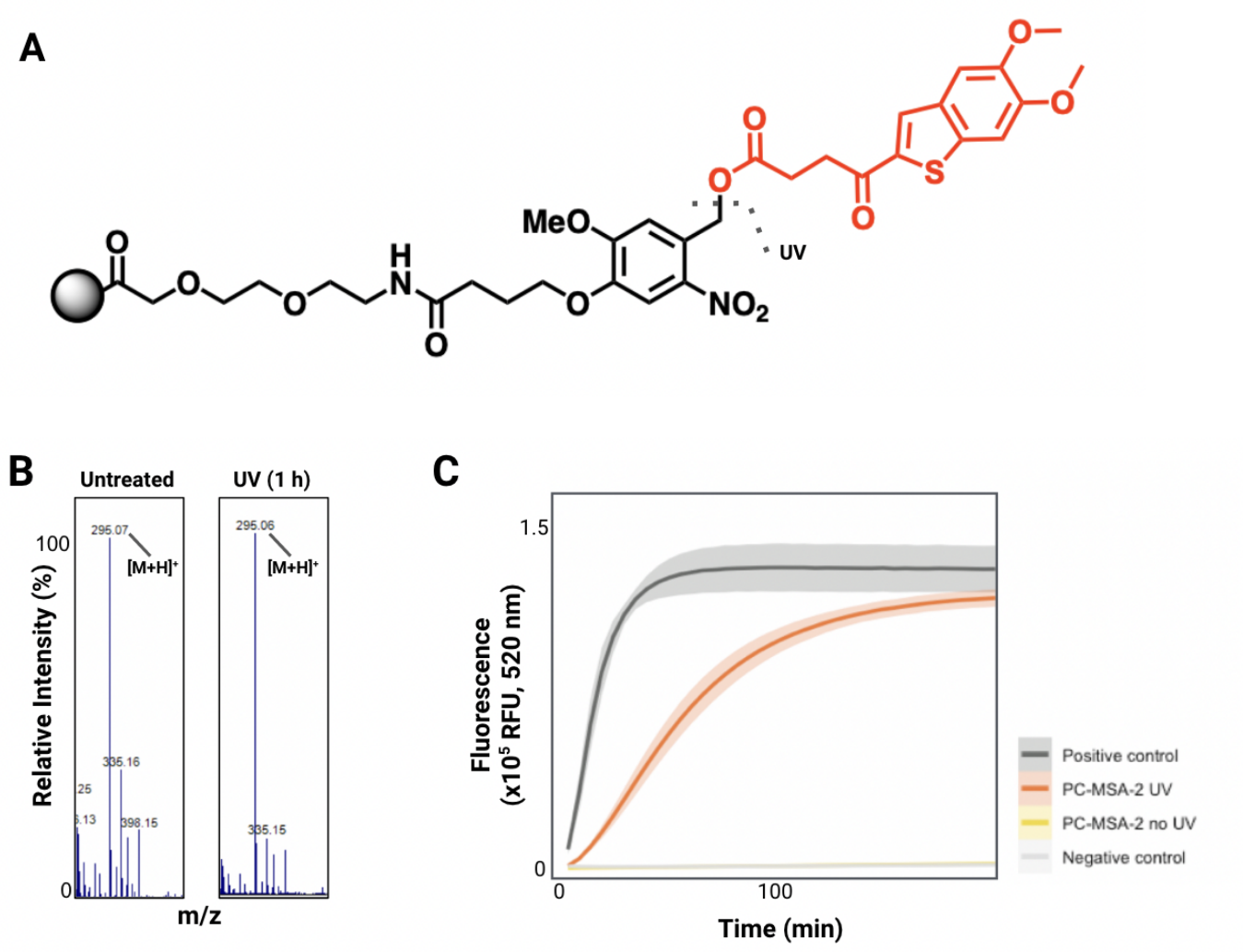

lack of signal change in the unirradiated cells shows that the liberation of MSA-2 is necessary for the cells to sense the agonist, and cells anchored to the microcarriers will not start signaling before UV exposure. The last missing step is capture of a reporter that is secreted by cells on microcarriers due to a payload from the microcarrier. To do this, an inducible cell line must be developed where the cells are induced by a STING agonist and secrete Halo-FP in response. While we successfully integrated a plasmid for constitutive secretion of GFP-Halo, integration of an inducible sequence is much more complex. Selection of a stable cell line involves stimulation with MSA-2 and selection of fluorescent populations. Additional validation of signal transduction in the STING pathway must be confirmed by western analysis. Nonetheless, proof-of-concept is now within grasp now that these feasibility studies are complete.

Conclusion and Future Directions

Through this project, we demonstrated the primary basis necessary for a cell-based DEL assay. First, the DEL bead was re-engineered into a microcarrier capable of reporter capture using a flexible polyacrylamide signaling scaffold put on through bulk bead emulsification. Next, a gelatin layer was crosslinked via genipin, and we observed consistent cell seeding and growth on these microcarriers. Microcarrier seeding was then adjusted to achieve singlet microcarriers with cell monolayers that would achieve one bead-one cell monolayer interactions. Next, we showed photodosage with a 385 longwave UV exposure over a prolonged period of time leads to high cell viability and acceptable photocleavage efficiency. Capture was established for microcarriers using a custom methacrylated HaloTag ligand that was incorporated into the polyacrylamide scaffold. These microcarriers were able to capture Halo-FP from a cell line we engineered to secrete Halo-FP constitutively. Lastly, we validated MSA-2 as our model STING agonist compatible with our assay conditions, and 293-Dual hSTING-R232 cells seeded onto photocleavable MSA-2 microcarriers were induced by UV liberation of MSA-2. These accomplishments together form the platform for a compartmentless cell-based DEL assay, but a mock screening with negative and positive control beads will validate the assay's viability.

In order to confirm the assay's viability, a mock screening with positive and negative control beads is necessary. Beads containing photocleavable MSA-2 would be seeded along with beads containing no payload. Liberation of compound should therefore expose cells on positive control beads to MSA-2, while cells on negative control beads experience negligible concentrations of MSA-2 in bulk. This experiment would confirm the existence of the proximity effect we predict using our secreted capture experiment and SEAP study, but necessitates an inducible cell line that can produce Halo-FP in response to MSA-2. We are limited as the R232 cells are proprietary with their mechanism for STING inducible response, and so the majority of the work in confirming this platform rests in production of this cell line.

Overall, this cell-based DEL platform shows a novel way to incorporate cells. Proof of compartmentless signaling allows assay flexibility with cells as long as microcarrier-microcarrier and cell-cell proximity is high and microcarrier-cell proximity is low. Our microcarrier formulation also imparts complex functionality, with desired modifications for cell seeding incorporated into the gelatin layer and modifications for capture and display incorporated into the polyacrylamide layer. Lastly, use of the STING agonist MSA-2 heralds this transition as able to target highly relevant disease targets, and means that any cell-based high throughput DEL screen should yield highly productive results. A reporter sequence based on any desired pathway target can be developed and inserted into cells, meaning translatability of this assay to other disease targets will be facile. We envision that this assay will be easily incorporated into workflows for DEL laboratories and pave the way for new druggable matter.

REFERENCES

[1] Clark, M. A.; Acharya, R. A.; Arico-Muendel, C. C.; Belyanskaya, S. L.; Benjamin, D. R.; Carlson, N. R.; Centrella, P. A.; Chiu, C. H.; Creaser, S. P.; Cuozzo, J. W.Design, Synthesis and Selection of DNA-Encoded Small-Molecule Libraries. Nat. Chem. Biol. 2009, 5, 647– 654, DOI: 10.1038/nchembio.211

[2] Adrián Gironda-Martínez, Etienne J. Donckele, Florent Samain, and Dario Neri. ACS Pharmacology & Translational Science 2021 4 (4), 1265-1279
DOI: 10.1021/acsptsci.1c00118

[3] Satz, Alexander L. “What Do You Get from DNA-Encoded Libraries?.” ACS medicinal chemistry letters vol. 9,5 408-410. 17 Apr. 2018, doi:10.1021/acsmedchemlett.8b00128

[4] Cochrane, Wesley G et al. “Activity-Based DNA-Encoded Library Screening.” ACS combinatorial science vol. 21,5 (2019): 425-435. doi:10.1021/acscombsci.9b00037

[5] Hackler, Amber L et al. “Off-DNA DNA-Encoded Library Affinity Screening.” *ACS combinatorial science* vol. 22,1 (2020): 25-34. doi:10.1021/acscombsci.9b00153

[6] Diana Castagna, David C. Budd, Simon J. F. Macdonald, Craig Jamieson, and Allan J. B. Watson. Journal of Medicinal Chemistry 2016 59 (12), 5604-5621
DOI: 10.1021/acs.jmedchem.5b01599

[7] Andrew B. MacConnell and Brian M. Paegel. ACS Combinatorial Science 2017, 19 (8), 524-532. DOI: 10.1021/acscombsci.7b00061

[8] Collins, D. J., Neild, A., deMello, A., Liu, A-Q., & Ai, Y. (2015). The Poisson distribution and beyond: Methods for microfluidic droplet production and single cell encapsulation. Lab on a Chip, 15(17), 3439 - 3459. https://doi.org/10.1039/c5lc00614g

[9] Derakhti, S.; Safiabadi-Tali, S. H.; Amoabediny, G.; Sheikhpour, M. Attachment and Detachment Strategies in Microcarrier-Based Cell Culture Technology: A Comprehensive Review. Mater. Sci. Eng. C 2019, 103, 109782. https://doi.org/10.1016/j.msec.2019.109782.

[10] John Kwon, Samuel F. Bakhoum; The Cytosolic DNA-Sensing cGAS–STING Pathway in Cancer. Cancer Discov 1 January 2020; 10 (1): 26–39.
https://doi.org/10.1158/2159-8290.CD-19-0761

[11] B.S. Pan, S.A. Perera, J.A. Piesvaux, J.P. Presland, G.K. Schroeder, J.N. Cumming, et al. An orally available non-nucleotide STING agonist with antitumor activity. Science, 369 (6506) (2020), p.eaba6098, 10.1126/science.aba6098

[12] Ferrari, C., Balandras, F., Guedon, E., Olmos, E., Chevalot, I. Limiting cell aggregation during mesenchymal stem cell expansion on microcarriers. Biotechnology Progress 2012 28 (3),780-787. https://doi.org/10.1002/btpr.1527

[13] Borys MC, Papoutsakis ET. Formation of bridges and large cellular clumps in CHO-cell microcarrier cultures: effects of agitation, dimethyl sulfoxide and calf serum. Cytotechnology. 1992; 8: 237–248.

[14] Van der Velden-deGroot C.A.M. (1995) Microcarrier technology, present status and perspective. In: Beuvery E.C., Griffiths J.B., Zeijlemaker W.P. (eds) Animal Cell Technology: Developments Towards the 21st Century. Springer, Dordrecht. https://doi.org/10.1007/978-94-011-0437-1_144

[15] C.L. Franco, J. Price, J.L. West. Development and optimization of a dual-photoinitiator, emulsion-based technique for rapid generation of cell-laden hydrogel microspheres. Acta Biomaterialia 2011, 7 (9), 3267-3276. https://doi.org/10.1016/j.actbio.2011.06.011.

[16] Rhutesh K., Ho Cheung Shum, Amy C. Rowat, Daeyeon Lee, Jeremy J. Agresti, Andrew S. Utada, Liang-Yin Chu, Jin-Woong Kim, Alberto Fernandez-Nieves, Carlos J. Martinez, David A. Weitz. Designer emulsions using microfluidics, Materials Today 2008 11 (4), 18-27. https://doi.org/10.1016/S1369-7021(08)70053-1.

[17] Maya Abdallah. Development of hydrogels and study the effect of their mechanical properties on podocyte behaviors. Material chemistry. Université Montpellier, 2019.

[18] Denisin AK, Pruitt BL. Tuning the Range of Polyacrylamide Gel Stiffness for Mechanobiology Applications. ACS Appl Mater Interfaces. 2016 Aug 31;8(34):21893-902. doi: 10.1021/acsami.5b09344. Epub 2016 Jan 27. PMID: 26816386.

[19] Georgyi V. Los, Lance P. Encell, Mark G. McDougall, Danette D. Hartzell, Natasha Karassina, et al.
ACS Chemical Biology 2008 3 (6), 373-382
DOI: 10.1021/cb800025k

[20] England, Christopher G et al. “HaloTag technology: a versatile platform for biomedical applications.” Bioconjugate chemistry vol. 26,6 (2015): 975-86. doi:10.1021/acs.bioconjchem.5b00191

[21] Tse, J.R. and Engler, A.J. (2010), Preparation of Hydrogel Substrates with Tunable Mechanical Properties. Current Protocols in Cell Biology, 47: 10.16.1-10.16.16. https://doi.org/10.1002/0471143030.cb1016s47

[22] Wen, Jessica H et al. “Interplay of matrix stiffness and protein tethering in stem cell differentiation.” Nature materials vol. 13,10 (2014): 979-87. doi:10.1038/nmat4051

[23] Flanagan, Lisa A et al. “Neurite branching on deformable substrates.” Neuroreport vol. 13,18 (2002): 2411-5. doi:10.1097/00001756-200212200-00007

[24] Wong, S.S. (1993) CRC Chemistry of Protein Conjugation and Crosslinking. CRC Press, Boca Raton, Florida.

[25] Syed, S., Karadaghy, A., Zustiak, S. Simple Polyacrylamide-based Multiwell Stiffness Assay for the Study of Stiffness-dependent Cell Responses. J. Vis. Exp. (97), e52643, doi:10.3791/52643 (2015).

[26] Habraken WJ, Boerman OC, Wolke JG, Mikos AG, Jansen JA. In vitro growth factor release from injectable calcium phosphate cements containing gelatin microspheres. J Biomed Mater Res A. 2009 Nov;91(2):614-22. doi: 10.1002/jbm.a.32263. PMID: 18985784.

[27] Adhirajan N, Shanmugasundaram N, Babu M. Gelatin microspheres cross-linked with EDC as a drug delivery system for doxycyline: development and characterization. J Microencapsul. 2007 Nov;24(7):647-59. doi: 10.1080/02652040701500210. PMID: 17763059.

[28] Solorio, L., Zwolinski, C., Lund, A.W., Farrell, M.J. and Stegemann, J.P. (2010), Gelatin microspheres crosslinked with genipin for local delivery of growth factors. J Tissue Eng Regen Med, 4: 514-523. https://doi.org/10.1002/term.267

[29] Righetti, P.G., Gelfi, C. and Bosisio, A.B. (1981), Polymerization kinetics of polyacrylamide gels. III. Effect of catalysts. ELECTROPHORESIS, 2: 291-295. https://doi.org/10.1002/elps.1150020507

[30] Klak, M et al. “Irradiation with 365 nm and 405 nm wavelength shows differences in DNA damage of swine pancreatic islets.” PloS one vol. 15,6 e0235052. 25 Jun. 2020, doi:10.1371/journal.pone.0235052

[31] Wong, Darice Y et al. “Low-Dose, Long-Wave UV Light Does Not Affect Gene Expression of Human Mesenchymal Stem Cells.” PloS one vol. 10,9 e0139307. 29 Sep. 2015, doi:10.1371/journal.pone.0139307

[32] Paige J. LeValley, Raghupathi Neelarapu, Bryan P. Sutherland, Srimoyee Dasgupta, Christopher J. Kloxin, and April M. Kloxin. “Photolabile Linkers: Exploiting Labile Bond Chemistry to Control Mode and Rate of Hydrogel Degradation and Protein Release”Journal of the American Chemical Society 2020 142 (10), 4671-4679
DOI: 10.1021/jacs.9b11564

[33] MacConnell, Andrew B et al. “An Integrated Microfluidic Processor for DNA-Encoded Combinatorial Library Functional Screening.” *ACS combinatorial science* vol. 19,3 (2017): 181-192. doi:10.1021/acscombsci.6b00192

[34] Gupta, Priyanka et al. “Optimization of agitation speed in spinner flask for microcarrier structural integrity and expansion of induced pluripotent stem cells.” Cytotechnology vol. 68,1 (2016): 45-59. doi:10.1007/s10616-014-9750-z

[35] Ran, F., Hsu, P., Wright, J. et al. Genome engineering using the CRISPR-Cas9 system. Nat Protoc 8, 2281–2308 (2013). https://doi.org/10.1038/nprot.2013.143

[36] Dou, Yuanyuan et al. “The CAG promoter maintains high-level transgene expression in HEK293 cells.” FEBS open bio vol. 11,1 (2021): 95-104. doi:10.1002/2211-5463.13029

[37] Hayashi, H., Kubo, Y., Izumida, M. et al. Efficient viral delivery of Cas9 into human safe harbor. Sci Rep 10, 21474 (2020). https://doi.org/10.1038/s41598-020-78450-8

[38] Krysten A. Jones, David J. Li, Elliot Hui, Mark A. Sellmyer, and Jennifer A. Prescher. Visualizing Cell Proximity with Genetically Encoded Bioluminescent Reporters.
ACS Chemical Biology 2015 10 (4), 933-938
DOI: 10.1021/cb5007773

[39] Weiss, Julia M et al. “The STING agonist DMXAA triggers a cooperation between T lymphocytes and myeloid cells that leads to tumor regression.” Oncoimmunology vol. 6,10 e1346765. 7 Jul. 2017, doi:10.1080/2162402X.2017.1346765

[40] B. Neises, W. Steglich, Simple Method for the Esterification of Carboxylic Acids Angew. Chem. Int. Ed., 1978, 17, 522-524.